

STUDENT EXERCISES AT DIAR POLIMI: DIGITAL AND ANALYTICAL METHODS FOR TARGET LOCATION AND DEM GENERATION

G. Forlani*, E.S. Malinverni**, L. Pinto**

*Dip. Ing. Civile - Università di Parma

**D.I.I.A.R. - Politecnico di Milano

ISPRS Commission VI - Working Group 3

Key words: LSM, DEM generation, Interpolation, Breaklines

ABSTRACT

This paper describes the survey of a fountain by the students during the exercises at Politecnico di Milano, comparing measurements made on an analytical plotter and on a digital workstation and showing the results of the surface reconstruction of the object.

The images were acquired by an analogue camera and then scanned: a two stage procedure for the determination of the interior orientation of digital images is discussed. The results of the block adjustment with the two data sets are presented.

A subset of images has been used to generate a DEM of the object surface. Points were selected by interest operators and measured by l.s.m. contemporarily in triplets of images, to provide reliability. Object boundaries and breaklines were interpolated by 3D curves defined by selected points, to reduce interpolation errors in the DEM. Finally, some remarks on 3D surface interpolation of complex objects are presented.

1. Student exercises in photogrammetry

Thanks to their small number (around 20-25 per year) there is scope for carrying out the survey of some object, to let the students have a concrete experience of a photogrammetric survey. The objectives we had in mind were:

- the design and the execution of the photogrammetric network;
- the comparison of digital and analytical techniques, when measuring signalized points;
- the reconstruction of the interior orientation of images digitized with DTP scanners;
- the bundle block adjustment;
- the reconstruction of the object surface by l.s.m. techniques.

1.1 Object characteristics

This year the choice fell on a granite fountain (see Fig. 1.1) nearby the Politecnico: it is a truly 3D object, with discontinuities and several hidden parts, good to test automatic methods. We left out of the survey the base and the top of the fountain (no safe platform available to take pictures at 4 m height!).



Figure 1.1 - The surveyed fountain

2. The design of the photogrammetric network

We wanted a block, running around the object, made up of a series of connected "trinocular models" with slightly convergent axes, to ensure the reliability much needed to automatic techniques.

A rough CAD model of the object has been derived from tape measurements. Based on this, camera stations have been placed and the visible object corners projected on each. Stations were set on a circle of 7 m radius, 30° apart each other, taking one shot with camera height set to 70 cm and a second one at 160 cm. A simulated block adjustment, run with a measurement accuracy of 6 μm, proved the scheme to be adequate.

Project objective	Constraints:
$\sigma_{\text{obj coord}} \leq 3 \text{ mm}$	Camera: Rollei 6006 - 50 mm lens Max height of the tripod (1.9 m) Max scan resolution: 600 dpi; no transparency module Measurement accuracy on digital images < 1/3 pixel

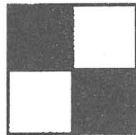
2.1 The control network

The ground control has been provided by multiple forward intersection with a T2 Wild theodolite from 3 stations, measuring the distances between stations by a horizontal rod. From each station, horizontal and vertical angles were measured to 6 targets; the accuracy for g.c.p. was better than 0.2 mm in XYZ.

2.2 Target dimensioning

Square targets (simply printed on paper) were used either for the control as well as for the tie points: their size has been dimensioned based on the following constraints:

- target size in the image: ~ 20 pixels;
- l.s.m. measurement accuracy: ~ 1/3 of pixel.



The target

To compute the distance to the object, the formula for the stereo normal case has been used: fixing the base to height ratio $Z/b = 1/2 \cotg(30^\circ)$ the unknown distance Z has been derived from:

$$\sigma_Z = \frac{Z^2}{b \cdot c} * \sigma_m$$

where:

- b = baseline
- c = principal distance = 50 mm
- Z = camera-object distance
- σ_m = image coordinates accuracy = 6 μ m

2.3 Image digitization

The required accuracy of image coordinates (6 μ m) corresponds to a pixelsize of about 20 μ m. Given the scanner characteristics (a HP scanner with maximum optical resolution of 600 dpi), an enlargement 2.8x was necessary and the actual scanning resolution was therefore set to 450 dpi. As far as the target size is concerned, since the minimum image scale is around 1:140 and the pixelsize of the digital images is 56 μ m, the target size was fixed to about 5.5 cm.

3. Image orientation

Measurements were performed on :

- an analytical stereoplotter Digicart 40 (by the operator);
- a Digital Photogrammetric Workstation (DPW) based on a Vax 3200 (automatically by l.s.m.)

3.1. Interior orientation

Image deformations due to lens distortion were corrected with data from the calibration certificate, while deformations due to film unflatness, shrinkage of printed copies and scanning by a DTP scanner were corrected by comparing the pixel and the image coordinates of the reseau crosses.

Using (semi)automatic methods to locate the reseau crosses, two needs should be taken into account (Forlani et al. 1996):

- a consistent but simplified model, to compute the global transformation from image to pixel system: this provides redundancy to identify blunders;
- a locally adaptive model, capable of maintaining continuity over image format: this provides a good local fitting.

The program implemented on the digital workstation follows the above mentioned approach:

- compute approximate location of all reseau crosses from 5 crosses measured manually;
- refine their position by template l.s.m.;
- determine a global affine transformation and perform blunder detection;
- compute a 8-parameters transformation for each reseau patch;
- applies the transformation from pixel to image coordinate system.

In the following table the results of the interior orientation are presented.

Test	Analytical Stereoplotter	Digital Workstation
Average # points measured	25/121	15/42
Measurement accuracy	4 μ m (manual)	0.05 pix 2.8 μ m (automatic)
Type of Transformation	Affine general (6 par.)	Projective (8 par.)
σ_0	30 μ m	0.48 pix * 27 μ m

* With affine general transformation

Table 3.1 - Interior orientation

3.2 Target measurement

The measurement of the targets has been performed manually on the Digicart and interactively, by template l.s.m., on the DPW. Automatic location of targets, which is easy using retroreflective targets, is possible but more difficult, since no simple thresholding can separate the background from the region of interest. Interaction is acceptable in this case, due to the small number of points per image; indeed it is almost necessary to assign the initial values to the shaping parameters of the l.s.m. where perspective deformations of the targets are high, in order to get high correlation values.

4 Block adjustment

To compare the two different image coordinate sets, two bundle block adjustments were carried out, using the program CALGE.

No additional tie points have been measured, since the target distribution and their number is even, though not always optimal.

Block adjustment was performed with minimum constraint; only one small blunder was found in the Digicart set, while in the DPW set there were no blunders.

Test	#Points Photo	Check points	Tie points	Eq. Un.	σ_0 [μm]	$\frac{\sigma_0}{\text{pix. size}}$	Tie points		Check points			
							σ_{xy} [mm]	σ_z [mm]	Empirical accuracy		Theoretical accuracy	
									RMS _{xy} [mm]	RMS _z [mm]	σ_{xy} [mm]	σ_z [mm]
Analytical Stereoplotter	15	4+3	36	368/198	7.4	-	2.4	1.3	4.8	0.8	2.1	1.2
Digital Workstation	13	4+3	36	300/198	6.0	0.11	2.8	1.3	0.8	0.1	2.3	1.2

Table 4.1 - Bundle block adjustment results

The relevant results of the block adjustment are shown in the Table 4.1; three full check points and one in height only were provided by the targets surveyed by the theodolite.

All sets show basically the same accuracy, with a slightly better empirical accuracy of the digital set. Nevertheless more targets could be successfully measured on the analytical plotter; moreover the time required by the digital measurements was significantly larger than on the analytical plotter because, in order to reach a sufficient correlation level, the assignment of initial values to the shape parameters took some time.

5. DEM generation

Given the orientation parameters of the images a l.s.m.-based procedure has been applied to generate a point cloud describing the object, to be approximated by suitable functions. The interpolation software available can only handle surfaces whose points are expressed as explicit functions $Z=Z(X,Y)$ of one of the variables: to complete the object survey therefore we should have broken the reconstruction in several parallel stages, each applied to part of the object surface, performing the reconstruction in a local reference system and finally combining all data in a common frame, which is easy thanks to the knowledge of the object coordinates of the tie points. Though the concept is straightforward, its implementation is time consuming. For the time being therefore, only one side of the fountain has been reconstructed.

The method (see Forlani et al. 1995 for details) is based on the simultaneous processing of three images (one acting as template) and makes use of the epipolar constraint. To further reduce the search space for homologous points, an initial very coarse DEM is estimated by any interpolation method (the nearest neighbour proved to be the most suited for a faithful representation in our case), using tie and control

points and a rough description of the object shape and its boundaries.

In an early stage, only six pictures were used (three from the upper and three from the lower ring of twelve), selecting any appropriate set of three images (see Fig. 5.1 (a)). Due to the significant convergence between optical axes, only adjacent pictures were used, to reduce scale changes and perspective distortions. Later, also the other six images were included, because there were significant portions of the object occluded in at least one image. This time we used triplets arranged at the vertices of a smaller triangle with a better geometry (see Fig. 5.1 (b)).

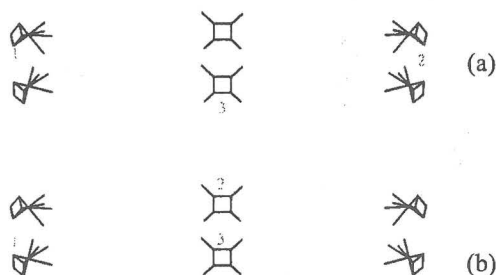


Fig. 5.1 - The two kinds of triplet of images used

Candidate points were selected either by an interest operator and at the nodes of a regular grid in object space and then transferred onto the other images and matched using an affine transformation. A triplet of image points was accepted based on two criteria:

- a correlation coefficient of the l.s.m. larger than 0.85;
- given the triangle whose vertices are determined by the intersection of each pair of image rays, if their average distance from the gravity centre was less than 1.5 mm.

This second criterium, which has been used successfully in the past, this time didn't performed well, leading to several mismatches, clearly visible as spikes emerging from an otherwise smooth object

surface. We couldn't find a clear explanation to this fact, but the reason may be the poor configuration of the triangle of the three projection centres of each triplet, which is far from a more ideal equilateral shape. Therefore the epipolar lines in the third image may not intersect each other at steep angles and the candidate point cannot be precisely located.

Several of these mismatches were nevertheless identified later by running a bundle adjustment separately for each triplet, where orientation parameters were kept fixed: this suggests that there may be possible ill configurations of the projective rays leading to a triangle in object space which is still small but far from the correct position. We plan to substitute the current consistency check on object coordinates with the computation of object coordinates in a single bundle adjustment of the triplet of rays.

At the end of the matching procedure, 7532 points were accepted as part of the point cloud for DEM generation. As can be seen from Fig. 5.2, the point distribution on the object is uneven, despite choosing different triplet of images: this is probably due to shadows for some areas and to lack of well defined features elsewhere, since the threshold for the correlation coefficient was set to a relatively high value.

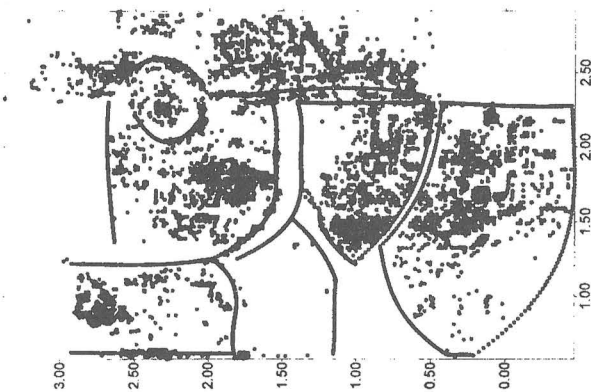


Fig. 5.2 - Point cloud and interpolated lines for DEM generation.

A serious problem arose from the lack of points found by the l.s. matching along object boundaries and discontinuities. In fact, interpolation by Delaunay triangulation or by the more sophisticated Kriging method lead to incorrect representation of the object, which is composed by several adjacent smooth blocks separated by large jumps (see Fig. 1.1), since they were not clearly defined in the data collected automatically. To force the interpolating surface through the boundaries it is necessary to explicitly assign the breaklines or to represent them as a very dense point sequence. To overcome this problem, points were selected manually by the operator along the object's edges in one template image and then input to the DEM generation program. The object points so found were interpolated by low order

polynomials to define the edges and the object boundaries. In such a way, 20 border lines were identified, to separate the different blocks; the result, shown in Fig. 5.3 (a) is still far from perfect or complete, due to the failure of the procedure along some boundaries, because of shadows or poor local contrast. Nevertheless, the faithfulness of the representation greatly improved after this stage, as it can be seen comparing Fig. 5.3 (a) and (b).

Even including breaklines, the choice of the interpolation method matters (see Fig.5.4), since some methods are better at handling discontinuities than others: no one provided by the current release of the package we used did perform well in this respect.

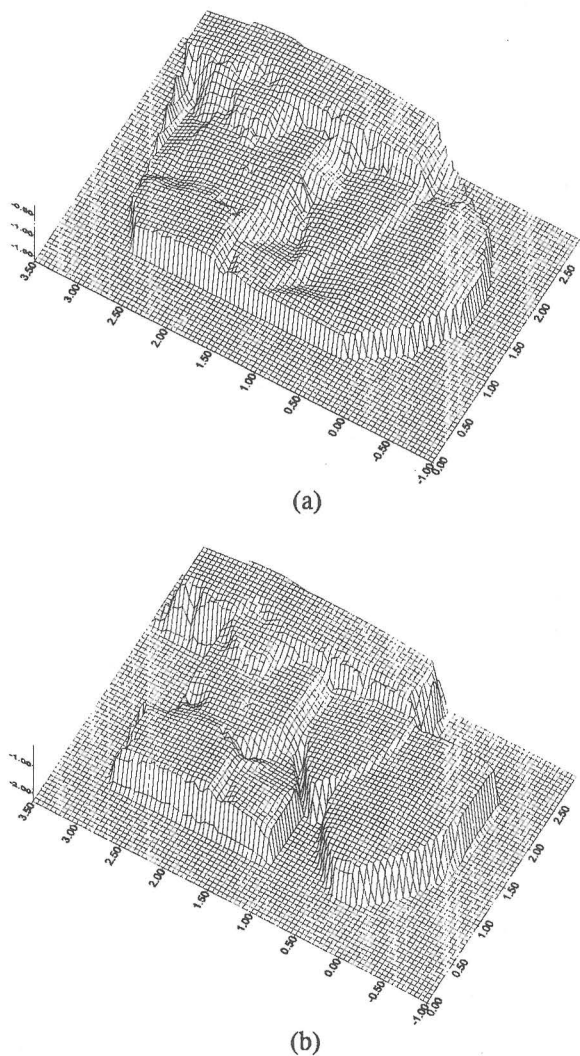


Fig. 5.3 - DEM without (a) and with (b) border lines

Due to random measurement errors and to a number of small blunders which still can be highlighted by visual inspection, the surface representation should be obtained by a smoothed function, allowing residuals on measurement points.

6. Prospects

As far as automation of the procedure is concerned, two main aspects emerge from the survey of this

fountain: the need for 3D extraction of object contours and the choice of an appropriate interpolation method.

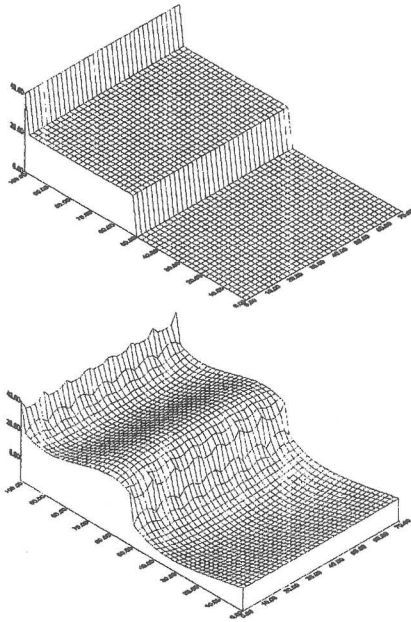


Fig. 5.4 - Interpolation of a step by triangulation (above) and kriging (below)

Automatic extraction of edges is feasible, but their matching in 3D is more complicated, even in case they are sharp and well defined: nevertheless there is a clear need for the inclusion of contour information to be integrated with the point cloud coming from l.s.m. In our case, where actually the faces of the blocks fountain are connected by smooth edges, so that what can be extracted by an edge operator in one image is likely to be different from that in the other images, due to change in viewpoint (see Fig. 6.1). To improve object description, such edges should be identified and a simple local model, e.g. describing object curvature, may be fitted.

More sophisticated interpolation methods should be used, at least in the final stages of the procedure, to represent the object surface including its breaklines; methods capable of detecting object discontinuities from the dataset should be preferred.

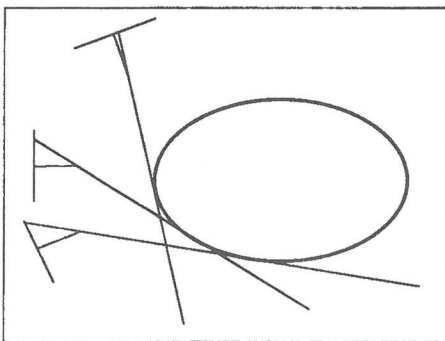


Fig. 6.1 - Edge mismatch due to occlusions

Acknowledgements

The authors are grateful to Marco Ferioli and Stefano Campi, who actually made most of the processing and measurements during their degree thesis.

References

- R. Al-Tahir, T. Schenk: *On the interpolation problem of automated surface reconstruction*. International Archives of Photogrammetry and Remote Sensing, vol. 29/3, Washington D.C., 1992
- Baltsavias E.P., 1991: *Multiphoto geometrically constrained matching*. Institut für Geodasie und Photogrammetrie, Mitteilungen n. 49, ETH, Zurich.
- Baltsavias, E.P. 1994: *Test and calibration procedures for image scanners*. International Archives of Photogrammetry and Remote Sensing, vol. 30/1, Como, 1994.
- Forlani G., Malinverni E.S., 1995: *DEM and orthophoto generation in close range photogrammetry*. Proc. of ISPRS TC1 Workshop "Multimedia GIS data", CISM, Udine (Italy).
- Forlani, Malinverni, Pinto, 1996: *A digital approach to the photogrammetric survey by reseau cameras*. In "Reports on surveying and geodesy (in memory of A. Gubellini and G. Folloni)", Nautilus, Bologna (Italy).
- Forlani G., Pinto L., Trebeschi A., 1995: *Measuring ground control points by l.s. matching*. In: Soft Computing in Remote Sensing Data Analysis. Binaghi, Brivio, Rampini (Ed's), Series in Remote Sensing, World Scientific, Singapore, 1996, p. 223-233.
- W. E. L. Grimson, T. Pavlidis, 1985: *Discontinuity Detection for Visual Surface Reconstruction*. Computer Vision, Graphics, and Image Processing n° 30, 1985.
- Kraus K., 1994: *Photogrammetry*. Wichmann Verlag.